4

The Analytic Form of the Daylight Locus

Geoffrey Iverson and Charles Chubb

It is an interesting computational exercise to take the full collection of Munsell chips, including the grays, illuminate them all with a standard source such as D_{65} or a flat equal energy source, present the reflected lights to three receptors following the spectral absorption profiles of human cones, integrate to produce receptor excitation 3-vectors, one vector per chip, and plot the totality of excitation vectors on a computer screen. What does one see?

Not much at first: a blob, a splotch with no apparent structure. However, as one zooms in on the blob and rotates appropriately, a structure appears. The excitation vectors corresponding to the same Munsell value (gray scale) fall in parallel planes, and within any such plane, the colors form nested chromatic loops (roughly, "ovoids"), each loop being distinguished by a different value of chroma (saturation). Qualitatively, the overall structure resembles a double-cone, just as one would expect if Munsell reflectances were well represented by the simplest Fourier basis 1, sin, cos.

What happens to this structure when one changes the illuminant? If the illuminants are the different phases of daylight, and the receptors are based on the Commission Internationale de l'Éclairage (CIE) 2deg color matching functions (Stockman & Sharpe, 2000; Stockman, Sharpe, & Fach, 1999), the constant (gray) reflectance moves along a three-dimensional curve, which when replotted in CIE chromaticity coordinates (x, y) is the *daylight locus*. This locus is known (Wyszecki & Stiles, 1982) to be well fit by a quadratic equation,

$$y_D = -3x_D^2 + 2.87x_D - 0.275.$$

In Figure 4.1 the circles represent, in CIE chromaticity coordinates, 12 phases of daylight equally spaced in reciprocal correlated color temperature (mired scale). The extreme points correspond to T_c = 4,000 K (upper right) and T_c = 25,000 K (lower left). The curve represented by the continuous line

DOI: 10.1037/14135-005
Human Information Processing: Vision, Memory, and Attention, C. Chubb, B. A. Dosher, Z.-L. Lu, and R. M. Shiffrin (Editors)

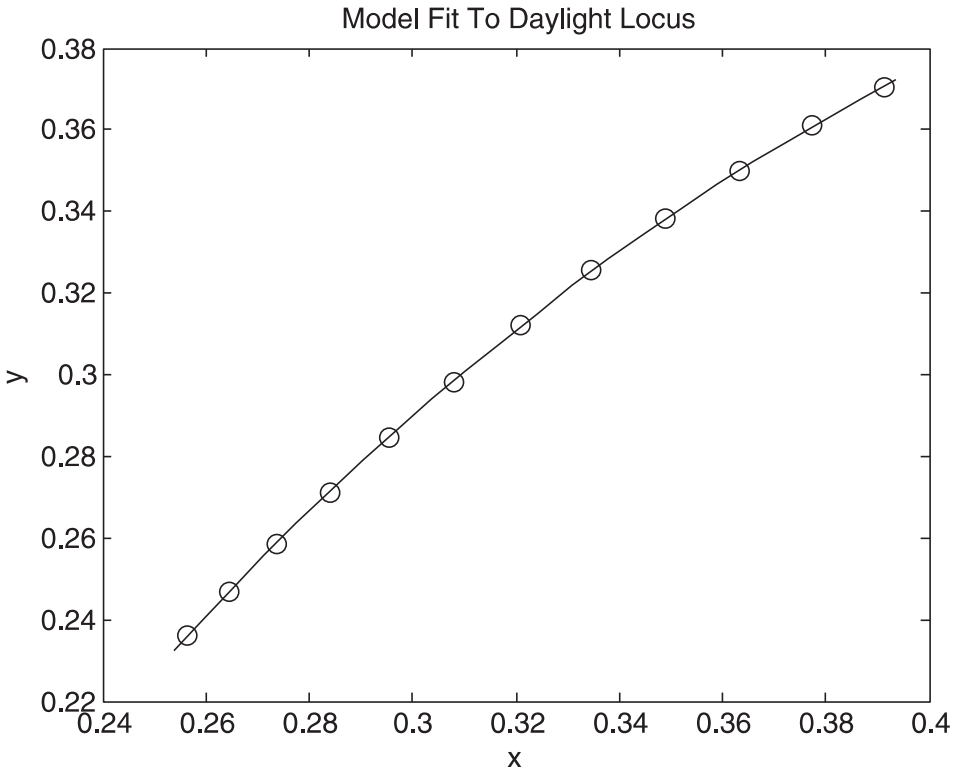

Figure 4.1. Twelve phases of daylight interpolated by an analytic function predicted to follow from a property of visual receptors. This property, which we call *similarity,* is discussed in detail later in the chapter.

interpolating these 12 daylights does *not* follow the empirically fit CIE quadratic but instead is a rather complicated implicit function of the form

$$x(u)=\frac{a+bu+cu^{\vartheta}}{A+Bu+Cu^{\vartheta}}, y(u)=\frac{a'+b'u+c'u^{\vartheta}}{A+Bu+Cu^{\vartheta}}, \qquad (4.1)$$

where *a, b, c, a′, b′, c′, A, B, C* and ϑ are all *known* constants, and *u* is the running coordinate of the locus; *u* is a positive number varying over an interval.

The curve expressed by Equation 4.1 is not an empirical template with 10 free parameters to be estimated from some fitting procedure. Rather, the 10 constants in Equation 4.1 are fixed by an underlying theory, developed later in the chapter, that is expressed most naturally not in CIE coordinates but in terms of cone excitations. Equation 4.1 looks relatively complicated only because the passage from cone excitations to the projective CIE chromaticity coordinates introduces that complexity. In contrast, when expressed in terms of ratios of cone excitations, the daylight locus is a simple power function, with an exponent that is determined by the wavelength of maximum sensitivity of each of the cones.

It seems a bit limp to expend so much effort on understanding the daylight locus as a curve in cone-excitation coordinates. Can we extend our theory of a

gray surface to chromatically selective surfaces? The answer is yes, and we briefly consider the extension in our concluding remarks. Although our theoretical developments are concentrated on a white surface, similar considerations apply to all Munsell chips.

To develop the theoretical basis for Equation 4.1, we proceed through a sequence of increasingly more realistic models for receptor excitations produced by daylights shining on a white surface. The simplest model we consider assumes narrowband photoreceptor sensitivities. Despite the obvious shortcomings of the narrowband assumption, it generates simple predictions that, to a surprising degree, are preserved in more realistic models. The narrow-band assumption yields a special case of the theoretically important *diagonal* model (Finlayson, Drew, & Funt, 1994; Forsyth, 1994), which predicts that surface ratios of these narrowband receptor excitations are invariant over changes in the illuminant spectral power distribution.

Now it turns out that to a good approximation, human cone excitation ratios are similarly invariant (Foster & Nascimento, 1994). Who would have anticipated this? We argue that the reason predictions of the narrowband model carry over to the broadband sensitivities characteristic of vertebrate photoreceptors resides in the similarity in shape of those receptor sensitivities (Lamb, 1995, 1999; Mansfield, 1985).

It is useful to consider in detail the predictions of a model that involves light from Wien illuminants absorbed by realistic photoreceptors (next section). In all of our calculations, we have used Stockman and Sharpe's (2000) estimates of the 2° human cone sensitivities. By *Wien illuminants,* we mean the family of spectral power distributions

$$W_T(\lambda) = c_1 \lambda^{-5} \exp\left(-\frac{c_2}{\lambda T}\right). \qquad (4.2)$$

Wien illuminants are close relatives of Planck (blackbody) radiators; the physical constants c_1 and c_2 are taken identical to those of the Planck radiation law (Wyszecki & Stiles, 1982); λ denotes wavelength (nm), and T denotes temperature (K). In calculations, we usually take in the range 4,000 K to 25,000 K to match the range of correlated color temperatures characteristic of daylights. However, the theory developed in the next section holds for a much larger range of temperatures, for example, $\infty \geq T \geq 3{,}000$ K.

Let us fix the notation that is in use throughout. We denote an arbitrary illuminant spectral power distribution by $E(\lambda)$. Special illuminants are given special notation: daylights are referred to by the notation $D_T(\lambda)$ and, as in Equation 4.2, Wien illuminants are written $W_T(\lambda)$. A general surface spectral reflectance function is denoted $R(\lambda)$. The daylight locus involves illuminating a surface whose reflectance spectrum is uniform, that is, $R(\lambda) = \text{constant}$, and the majority of our theoretical developments might seem to be irrelevant to colored surfaces. However, as already mentioned, our developments do, in fact, extend to colored surfaces (see the Conclusion section of this chapter).

Photoreceptor absorption spectra are denoted $S_k(\lambda)$, $k = L, M, S$; these are assumed to be normalized to take the value 1 at their maxima, which occur at

wavelengths λ_k, $k=L, M, S$. Photoreceptor excitations, denoted q_k, and produced by light reflected from a matte surface R lit by an illuminant E are given by

$$q_k(E,R)=\int_0^\infty E(\lambda)R(\lambda)S_k(\lambda)d\lambda,\ k=L,M,S \qquad (4.3)$$

We will often take logarithms of photoreceptor sensitivities. When we do so, we find it convenient to write $Q_k = \ln q_k$.

Narrowband Photoreceptors

In a simple model (Finlayson et al., 1994; Finlayson & Hordley, 2001; Marchant & Onyango 2001; Marchant & Onyango, 2002), it is assumed that photoreceptors are so narrowband as to be well represented by delta functions, that is, $S_k = \delta(\lambda - \lambda_k)$. In terms of the photoreceptor excitations given in Equation 4.3, the narrowband assumption entails that $q_k(E, R) = E(\lambda_k)R(\lambda_k)$. In vector notation, this model couples the excitation 3-vectors $\boldsymbol{q}(E, R)$ and $\boldsymbol{q}(E', R)$ by a diagonal matrix with nonzero elements that contain the ratios $E(\lambda_k)/E'(\lambda_k)$. This is the diagonal model referred to earlier. For future reference, we note here that the diagonal model is simple to interpret in logarithmic coordinates: under a change in illumination, $E \rightarrow E'$, all logarithmic excitation vectors $\boldsymbol{Q} = \log \boldsymbol{q}$ undergo a common rigid translation: $\boldsymbol{Q} \rightarrow \mathrm{Q}' = \mathrm{Q} + \boldsymbol{t}$ where $t_k = \log\left(\frac{E'(\lambda_k)}{E(\lambda_k)}\right)$. For a spectrally flat reflectance function—an ideal white surface—the kth photoreceptor excitation value is proportional to $E(\lambda_k)$, the value of the illuminant spectral power distribution evaluated at the peak wavelength λ_k of S_k.

When the illuminants are chosen from a one-parameter family such as Planck (blackbody) radiators, Wien illuminants, or Daylights, the excitations q_k trace out a space curve that is characteristic of the class of illuminants. In the special case of the Wien family of illuminants given by Equation 4.2, the coordinates of the Wien curve $T \mapsto (q_L(T), q_M(T), q_S(T))$ take on the especially simple form

$$q_k(T) = c_1\lambda_k^{-5}\exp\left(-\frac{c_2}{\lambda_k T}\right). \qquad (4.4)$$

It is evident from Equation 4.4 that color temperature T can be eliminated, allowing any two photoreceptor excitations to be expressed in terms of a third. In particular we have, for all excitations q_k on the Wien curve,

$$q_k = \rho_k \rho_L^{-\beta k} q_L^{\beta k} \text{ for } k=L,M,S, \qquad (4.5)$$

in which we have written $\rho_k = c_1\lambda_k^{-5} = \lim_{T\rightarrow\infty} q_k(T)$ and $\beta_k = \lambda_L/\lambda_k$. Thus, on the Wien curve, the M-cone excitation value is a power function of the L-cone excita-

tion value; the exponent $\beta_M = \lambda_L/\lambda_M$ of this power function is the ratio of the peak wavelengths of the two types of cones. Similarly, the S-cone excitation value is a power function of the L-cone excitation value, with exponent $\beta_M = \lambda_L/\lambda_S$.

It is useful to introduce projective coordinates $v = q_S/q_L$ and $u = q_M/q_L$ because these are independent of the intensity of illumination. A little algebra reveals that

$$v = \rho_L^{\vartheta-1}\rho_M^{-\vartheta}\rho_S u^{\vartheta}, \qquad (4.6)$$

in which the exponent ϑ is given by

$$\vartheta = \left(\frac{\lambda_L}{\lambda_S} - 1\right) \Big/ \left(\frac{\lambda_L}{\lambda_M} - 1\right) = \left(\frac{1}{\lambda_S} - \frac{1}{\lambda_L}\right) \Big/ \left(\frac{1}{\lambda_M} - \frac{1}{\lambda_L}\right). \qquad (4.7)$$

A useful alternative form of Equation 4.6 uses logarithmic coordinates. Recalling the definition of u and v, and taking logarithms in Equation 4.6, we have the *linear* equation

$$Q_S - Q_L = \eta + \vartheta(Q_M - Q_L), \qquad (4.8)$$

in which the slope ϑ and intercept η are dimensionless constants; ϑ is given in Equation 4.7, and $\eta = 5(\vartheta \ln(\lambda_M/\lambda_L) - \ln(\lambda_S/\lambda_L))$.

Alternative coordinates to are provided by the *chromaticities* introduced by MacLeod and Boynton (1979)—namely, $x = q_L/(q_L + q_M)$ and $y = q_S/(q_L + q_M)$. In these coordinates, the power function in Equation 4.5 becomes

$$y = Cx^{1-\vartheta}(1-x)^{\vartheta}, \qquad (4.9)$$

in which the constant $C = \rho_L^{\vartheta-1}\rho_M^{-\vartheta}\rho_S$.

This toy model, with its unrealistic photoreceptors, provides a poor basis for biological color vision. Nevertheless, we shall see later that its predictions are met, with surprising precision, under more realistic assumptions on photoreceptoral sensitivities. For future reference, we record here the value of the exponent ϑ assuming realistic photoreceptors. For human cones, Sharpe, Stockman, Jägle, and Nathans (1999) estimated $\lambda_L = 559.1$ *nm*, $\lambda_M = 530.6$ *nm* and $\lambda_S = 420.8$ *nm*. Using Equation 4.7, these values give $\vartheta = 6.12$. That value of ϑ is used to evaluate our prediction Equation 4.1 for the CIE daylight locus. We justify this numerical value for ϑ outside of the limitations of the narrowband model.

Photoreceptors With a Common Shape

The predictions expressed in Equations 4.6 through 4.9 of the narrowband model are, to an excellent approximation, preserved in a more realistic model using photoreceptors with mutually overlapping bandwidths, as is the case for vertebrate photoreceptors. This agreeable circumstance is a consequence of the

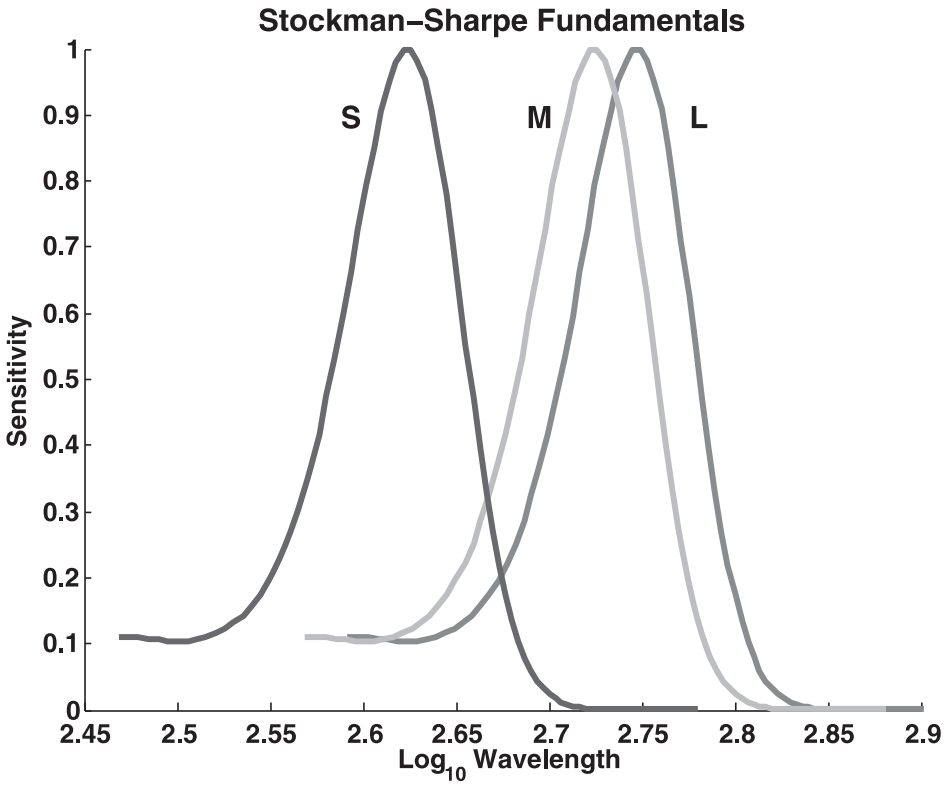

Figure 4.2. Stockman-Sharpe (Stockman & Sharpe, 2000) cone sensitivities plotted as functions of log wavelength. That these sensitivities are simple translations of one another means that they are similar in the sense of Equation 4.10 and footnote 1.

assumption that the photoreceptor sensitivities appear to be based on a *common* template. Specifically, we assume that as functions of log wavelength the photoreceptor sensitivities differ only in the values of their peak wavelengths. In other words,

$$S_k(\lambda) = S_{k'}(\lambda(\lambda_{k'}/\lambda_k)) \text{ for any indices } {}_{k,k' \in \{L,M,S\}}. \qquad (4.10)$$

The similarity[1] of photoreceptors formalized in Equation 4.10 is a striking feature of vertebrate photoreceptor sensitivities, including, of course, those of human rods and cones (Lamb, 1995; Mansfield, 1985). It is the similarity of cone sensitivities that allows the excitations of one class of cone to be related to those of any other class (cf. Equation 4.5), as we now show. The Stockman and Sharpe (2000) cone sensitivities are pictured in Figure 4.2. As functions of log wavelength, they are merely translations of one another.

[1]Let $\mathsf{F} = \{f_j(x) \mid j = 1, 2, \ldots, J\}$ be a finite collection of real-valued functions defined on the positive reals. We say that the collection F is *similar,* or equivalently that the functions $f_1, f_2, \ldots, f_J$ are mutually similar, if there are positive constants a_j, b_j and a function g such that $f_j(x) = a_j g(b_j x)$. If a family F is similar, it follows that all members of F can be expressed in terms of any single member, f_i, say, as follows: $f_j(x) = (a_j/a_i) f((b_j/b_i)x)$.

Excitations produced by shining a Wien illuminant on the photoreceptors are given by

$$q_k(T) = c_1 \int_0^\infty \lambda^{-5} \exp\left(-\frac{c_2}{\lambda T}\right) S_k(\lambda)\, d\lambda. \qquad (4.11)$$

We combine Equations 4.10 and 4.11 to express the excitations of the *M* and *S* photoreceptors in terms of those of the *L* receptors. It is enough to carry out the argument explicitly for the *M* excitations:

$$q_M(T) = c_1 \int_0^\infty \lambda^{-5} \exp\left(-\frac{c_2}{\lambda T}\right) S_M(\lambda)\, d\lambda$$

$$= c_1 \int_0^\infty \lambda^{-5} \exp\left(-\frac{c_2}{\lambda T}\right) S_L(\lambda\beta_M)\, d\lambda,$$

where $\beta_M = \lambda_L/\lambda_M$. By a simple change of variable, we obtain

$$q_M(T) = \beta_M^4 c_1 \int_0^\infty \lambda^{-5} \exp\left(-\frac{c_2}{\lambda T/\beta_M}\right) S_L(\lambda)\, d\lambda,$$

and we see that

$$q_M(T) = \beta_M^4 q_L(T/\beta_M). \qquad (4.12a)$$

In the same way, we have

$$q_S(T) = \beta_S^4 q_L(T/\beta_S), \qquad (4.12b)$$

where $\beta_S = \lambda_L/\lambda_S$. The ratios β_S and β_M are in constant use subsequently.

Equation 12a and 12b allow the Wien space curve $T \mapsto (q_L(T), q_M(T), q_S(T))$ to be expressed solely in terms of the excitations of any one of the photoreceptors, say, the *L*-cones. Put another way, the mutual similarity of photoreceptors as functions of wavelength λ is reexpressed (via the integration in Equation 4.11) as mutual similarity of the excitations q_k as functions of the Wien temperature T.[2]

By studying the function $T \mapsto q_L(T)$ in further detail, it is possible to develop an analogue of the system of Equation 4.5. Consider the *L*-excitations. We have[3]

[2]This transfer of similarity from functions of wavelength to functions of color temperature is not restricted to Wien illuminants. It holds as well for Planck blackbody radiators and in fact for any family of illuminants of the form $E(\lambda, T) = \lambda^{-\gamma} G(\lambda T)$.

[3]The existence of the function $T \mapsto \Lambda_L(T)$ arising in the second line of Equation 4.13 follows from the fact (an integral form of the mean-value theorem of the calculus) that for any functions f and g on a bounded open real interval I, f everywhere positive and g continuous on I, there exists $c \in I$ such that $\int_I g(x)f(x)dx = g(c)\int_I f(x)dx$.

$$q_L(T) = c_1 \int_0^\infty \lambda^{-5} \exp\left(-\frac{c_2}{\lambda T}\right) S_L(\lambda) d\lambda$$
$$= \exp\left(-\frac{c_2}{\Lambda_L(T) T}\right) c_1 \int_0^\infty \lambda^{-5} S_L(\lambda) d\lambda \qquad (4.13)$$
$$= \exp\left(-\frac{c_2}{\Lambda_L(T) T}\right) \rho_L .$$

In the last line of Equation 4.13, we have written $\rho_L = c_1 \int_0^\infty \lambda^{-5} S_L(\lambda) d\lambda = \lim_{T \to \infty} q_L(T)$. A graph of the function $T \mapsto \Lambda_L(T)$ (assuming the $S_L(\lambda)$ are the 2° spectral sensitivities of human *L*-cones given by Stockman and Sharpe, 2000) is shown in Figure 4.3 (top panel).

From Equation 4.13, we have

$$q_L(T/\beta_M) = \rho_L \exp\left(-\frac{c_2 \beta_M}{\Lambda_L(T/\beta_M) T}\right)$$
$$= \rho_L \left[\exp\left(-\frac{c_2}{\Lambda_L(T) T}\right)\right]^{\alpha_M(T)}$$
$$= \rho_L^{1-\alpha_M(T)} q_L^{\alpha_M(T)} .$$

The exponent $\alpha_M(T)$ is given by

$$\alpha_M(T) = \beta_M \frac{\Lambda_L(T)}{\Lambda_L(T/\beta_M)} . \qquad (4.14a)$$

From Equation 4.12a, we thus obtain

$$q_M(T) = \beta_M^4 \rho_L^{1-\alpha_M(T)} q_L(T)^{\alpha_M(T)} . \qquad (4.15a)$$

In the same way, we have

$$q_S(T) = \beta_S^4 \rho_L^{1-\alpha_S(T)} q_L(T)^{\alpha_S(T)} , \qquad (4.15b)$$

in which the exponent $\alpha_S(T)$ is given by

$$\alpha_S(T) = \beta_S \frac{\Lambda_L(T)}{\Lambda_L(T/\beta_S)} . \qquad (4.14b)$$

The Equations 4.15a and 4.15b correspond to the relations given in Equation 4.5 for $k = M, S$, respectively. The major difference, of course, between the two systems of Equations 4.5 and 4.15a–4.14b is that for the latter system, the exponents $\alpha_M(T)$ and $\alpha_S(T)$ depend on T through the factors $\frac{\Lambda_L(T)}{\Lambda_L(T/\beta_M)}$ and $\frac{\Lambda_L(T)}{\Lambda_L(T/\beta_S)}$. However, these factors vary but little in T for

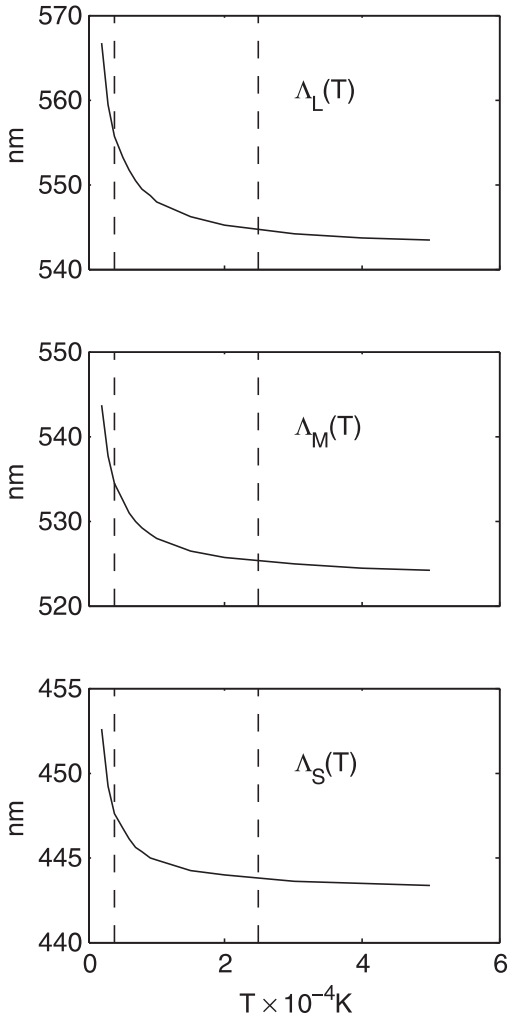

Figure 4.3. Characteristic wavelength functions $\Lambda_k(T)$, $k = L, M, S$ for a white surface. See the text for details, especially Equations 4.13 and 4.16. Notice that these functions are roughly constant except for small values of T (note the vertical scale in each plot). That these functions are mutually similar is established in Equation 4.18 and is also visually apparent. The dashed vertical lines delineate the set of Wien illuminants, $4{,}000 \leq T \leq 25{,}000$.

$T \geq 4000$ K (see Figure 4.3); and, to a good first approximation, they can be taken as constants. In turn, this means that taking logarithms in Equations 4.15a and 4.15b should produce nearly linear plots of Q_M vs. Q_L and Q_S vs. Q_L with respective slopes α_M and α_S. That this is, indeed, the case is shown in Figure 4.4.

An alternative path connecting Equations 4.12a and 4.12b and 4.15a and 4.15b proceeds by defining individual characteristic wavelength functions $\Lambda_k(T)$, one for each cone type:

$$q_k(T) = \rho_k \exp\left(-\frac{c_2}{\Lambda_k(T)T}\right), \qquad (4.16)$$

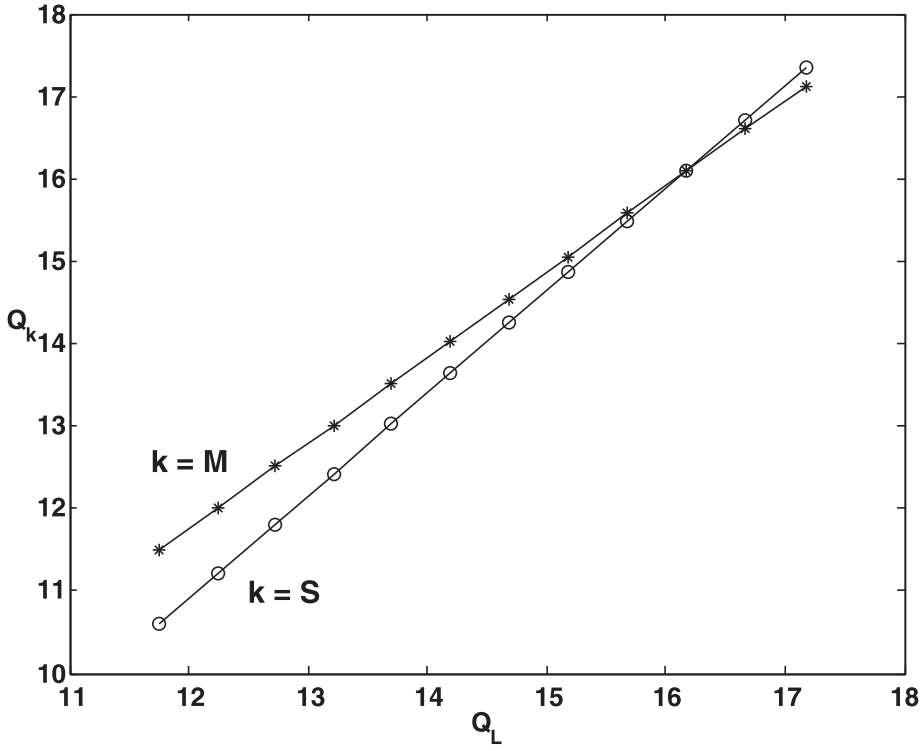

Figure 4.4. Log-excitation of M and S cones versus log-excitation of L cones. Variation in cone excitation is caused by variation in the temperature T of Wien illuminants shone on a white surface.

where $\rho_k = \lim_{T\to\infty} q_L(T)$. It follows that

$$q_k(T) = \rho_k \left(q_L(T)/\rho_L\right)^{\frac{\Lambda_L(T)}{\Lambda_k(T)}}. \qquad (4.17)$$

Comparing Equations 4.15a–4.15b and 4.17, we obtain

$$\Lambda_k(T) = \beta_k^{-1}\Lambda_L(T/\beta_k), _{k=L,M,S}. \qquad (4.18)$$

Thus, the mutual similarity of the cone sensitivities is again reflected in the mutual similarity of a different collection of functions—namely, the $\Lambda_k(T)$; compare Equations 4.18 and 4.12a–4.12b.

The Daylight Locus

Let us acknowledge two limitations of the foregoing developments that might conceivably have a negative impact on the conclusions of the previous section.[4]

[4]This section can be skipped at a first reading. The effects of optic media and the high frequency tail of daylight spectra on our theoretical developments are, in a sense, mere distractions.

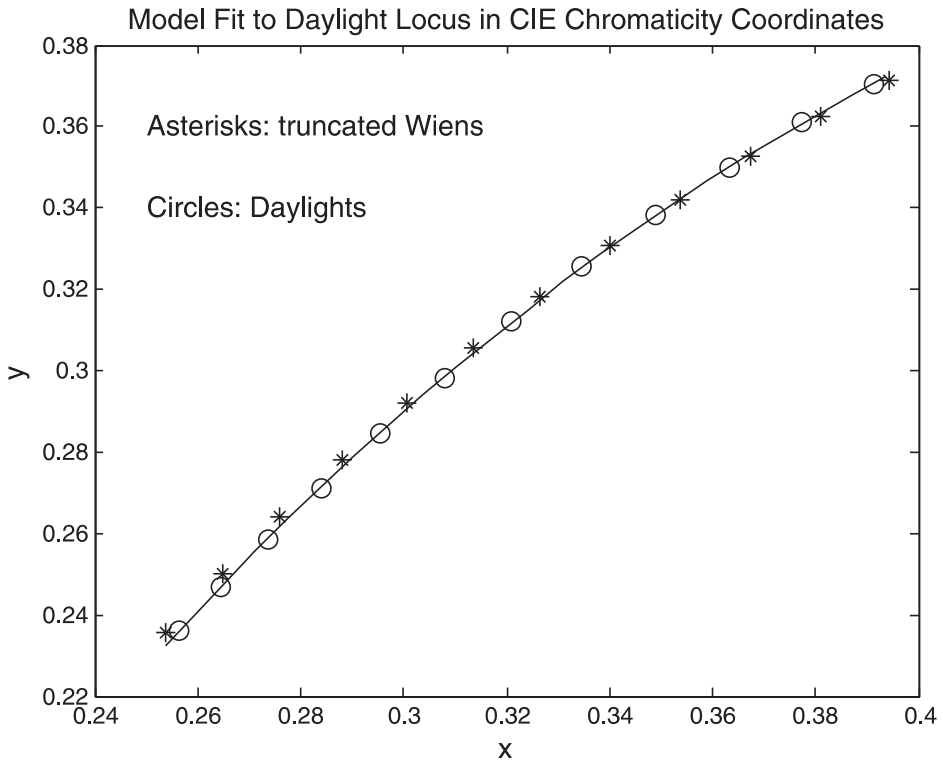

Figure 4.5. The daylight locus (open circles) and the locus of truncated Wien illuminants (asterisks).

On the one hand, we are interested in the daylight locus, and Wien illuminants are not identical to daylights. On the other hand, we have ignored the fact that the similarity property Equation 4.9 holds well for cones in vitro and not so well for corneal cone sensitivities; to deal with the latter, we need to take into account the optic media of the eye, primarily the macular pigment and the lens.

Fortunately, neither of these complications turns out to have important qualitative implications for the results established in the previous section. If one plots both the daylight locus and the corresponding Wien locus using coordinates $\ln(q_S/q_L) = Q_S - Q_L$ and $\ln(q_M/q_L) = Q_M - Q_L$, both loci plot as nearly parallel lines displaced from one another by approximately 0.1 log units. To make these loci more nearly superimpose, we alter the Wien illuminants so that they better approximate daylights. We do this by truncating the Wien spectra at short wavelengths.

Figure 4.5 is a plot in chromaticity coordinates of the daylight locus and the locus of truncated Wien illuminants; the two loci are now nearly coincident. That is, truncated Wien illuminants approximate daylights, and what has been shown analytically to hold for Wien illuminants carries over to the more complex daylight spectra.

To extend the theory in the previous section to incorporate the joint effects of the optic media and the truncation of the Wien illuminants, we note that these

two effects are of a similar nature. Each involves multiplication of the in vitro cone sensitivities by a wavelength transmittance function that is constant for wavelengths at or above 600 nm, decreasing to zero at short wavelengths. We can incorporate the effects of the optic media and the truncation of the Wien illuminants as a single transmittance $t(\lambda)$ rising from zero at or below 400 nm, and saturating with value 1 at approximately 600 nm. The appropriate generalization of Equation 4.10 is thus

$$q_k(T) = c_1 \int_0^\infty t(\lambda)\lambda^{-5} \exp\left(-\frac{c_2}{\lambda T}\right) S_k(\lambda) d\lambda. \qquad (4.19)$$

By the mean value theorem, the function $t(\lambda)$ can be taken out from the integral in Equation 4.19, and we have

$$q_k(T) = t(w_k(T)) c_1 \int_0^\infty \lambda^{-5} \exp\left(-\frac{c_2}{\lambda T}\right) S_k(\lambda) d\lambda.$$

The theoretical developments of the chapter's previous section now apply unchanged to the ratios $q_k(T)/t(w_k(T))$. We see that

$$\begin{aligned} q_k(T) &= \left(t(w_k(T))/t(w_L(T))^{\alpha_k(T)}\right) \beta_k^4 \rho_L^{1-\alpha_k(T)} q_L{}^{\alpha_k(T)} \qquad (4.20) \\ &= B_k(T) q_L(T)^{\alpha_k(T)}. \end{aligned}$$

The functions $B_k(T)$ and $\alpha_k(T)$ are slowly varying in T, and, to a good approximation, each is effectively constant over the range of values of T that define the daylight locus—namely, 4,000 K ≤ T ≤ 25,000 K. To a good approximation, the conclusions of the chapter's previous section are unchanged by the additional complications of the optic media.

Conclusion

We have shown that in appropriately chosen coordinates, for example, $(Q_M - Q_L, Q_S - Q_L)$, the daylight locus plots as a straight line. Moreover, the parameters of this line, and its direction in particular, are found to be determined by the peak sensitivities of the photoreceptors. This occurs because the cones are similar to one another in spectral shape. Because of this similarity, the cones behave in important respects as though they were narrowband receptors.

We have focused on the cone excitations produced by shining one-parameter families of illuminants (daylights, Wien illuminants, blackbody radiators) on a "white," spectrally flat piece of paper. This invites the following question: What happens if we replace our white piece of paper next to a colored one with a nontrivial reflectance spectrum $R(\lambda) \neq$ const. ? Suppose a member of the Wien family of illuminants is reflected from a surface with reflectance $R(\lambda)$, and the reflected light is absorbed by each cone type. The excitations produced are

$$q_k(R,T) = c_1 \int_0^\infty \lambda^{-5} \exp\left(-\frac{c_2}{\lambda T}\right) R(\lambda) S_k(\lambda) d\lambda,$$

and we can write this integral as

$$\begin{aligned} q_k(R,T) &= \bar{R}_k(T) c_1 \int_0^\infty \lambda^{-5} \exp\left(-\frac{c_2}{\lambda T}\right) S_k(\lambda) d\lambda \\ &= \bar{R}_k(T) q_k(1,T), \end{aligned}$$

where $\bar{R}_k(T)$ is an average value characteristic of the surface and the illuminant temperature T. Taking logarithms, we see that

$$Q_k(R,T) = \log \bar{R}_k(T) + Q_k(1,T).$$

It is clear that information about colored surfaces is carried by deviations from the white surface:

$$\Delta Q_k(R,T) = Q_k(R,T) - Q_k(1,T) = \log \bar{R}_k(T).$$

In Figure 4.6, we have plotted the loci of a chromatic loop of Munsell chips of the same saturation (chroma). We see that as illuminant temperature varies, each chip travels on a line with parameters that are characteristic of the color of the chip. Figure 4.6 is consistent with the idea that the vector of log excitations for any colored surface and any illuminant temperature T with $T_0 \le T \le T_1$, linearly interpolates between two standard "views," corresponding to (arbitrarily chosen) extreme color temperatures T_0 and T_1:

$$Q_k(R,T) = \phi(T) Q_k(R,T_0) + (1-\phi(T)) Q_k(R,T_1), \qquad (4.21)$$

with $0 \le \phi(T) \le 1$ and $\phi(T_0) = 1$. Evidently, the relative coordinates $\Delta Q_k(R, T)$ carrying chromatic information also satisfy Equation 4.21. This model is different from but closely related to the diagonal model (Finlayson et al., 1994; Forsyth, 1994; Foster & Nascimento, 1994). In addition, MacLeod and Golz (2003) presented an interesting Gaussian world that provides linear coordinates when expressed in logarithmic receptor excitation space, although in that world the motion of a white surface under changing illumination is along a quadratic curve rather than a line.

In logarithmic form, the diagonal model reads

$$Q_k(R,T) = A_k(R) + B_k(T). \qquad (4.22)$$

As we mentioned earlier, the defining property of the diagonal model is that it separates the effect of surface spectra R from the effect of the illuminant temperature T. The effect of changing illuminant temperature from T to T' is thus to translate all log-excitation vectors $\boldsymbol{Q}$ to new positions $\boldsymbol{Q}'$, and the translation vectors $\boldsymbol{Q}'$-$\boldsymbol{Q}$ do not depend on the surface reflectance spectrum R.

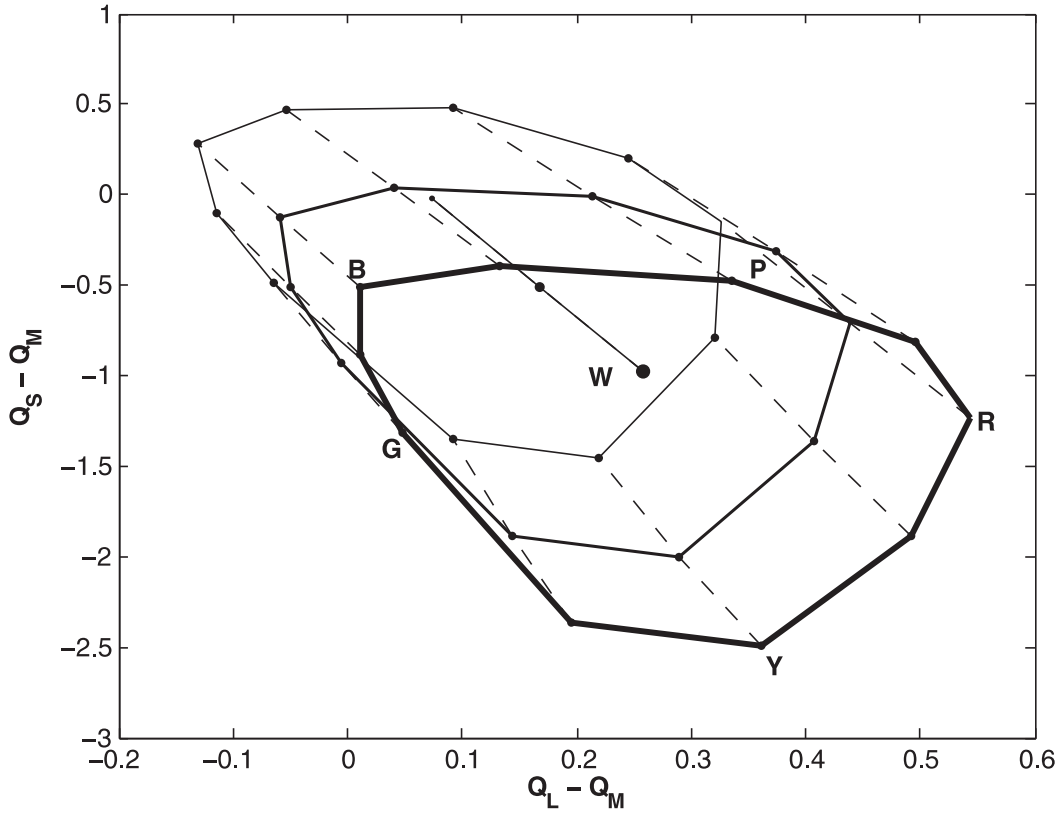

Figure 4.6. In logarithmic coordinates Munsell chips vary linearly with Wien temperature T. The larger chromatic loop closest to the viewer corresponds to $T = 4000$ K, the middle loop is for $T = 6{,}000$ K, and the smallest loop is for $T = 15{,}000$ K. The daylight locus is shown by the line connecting solid dots at the "center" of each loop.

The mixture weights $\phi(T)$ in Equation 4.21 can be expressed as

$$\phi(T) = \frac{Q_k(R, T_1) - Q_k(R, T)}{Q_k(R, T_1) - Q_k(R, T_0)}. \qquad (4.23)$$

That the ratio on the right-hand term of Equation 4.23 is independent of surface R and of cone type constitutes a remarkable prediction of the model expressed in Equation 4.21. This prediction is tested in Figure 4.7 and, as can be seen, it is well supported. Note, however, that dilatation (a noticeable "shrinking") with increasing T is evident in Figure 4.6. This dilatation is enough to rule out the diagonal model Equation 4.22.

We do not pursue any further in this chapter a more complete description of the transformations that move the gamut of Munsell chips along the daylight locus. We do note, however, that a prediction of Golz and MacLeod (2002) and MacLeod and Golz (2003) is obtained as a by-product of a more detailed description of our analysis: *As the light gets redder, the reds get lighter.* That this prediction is borne out in perception is easy to demon-

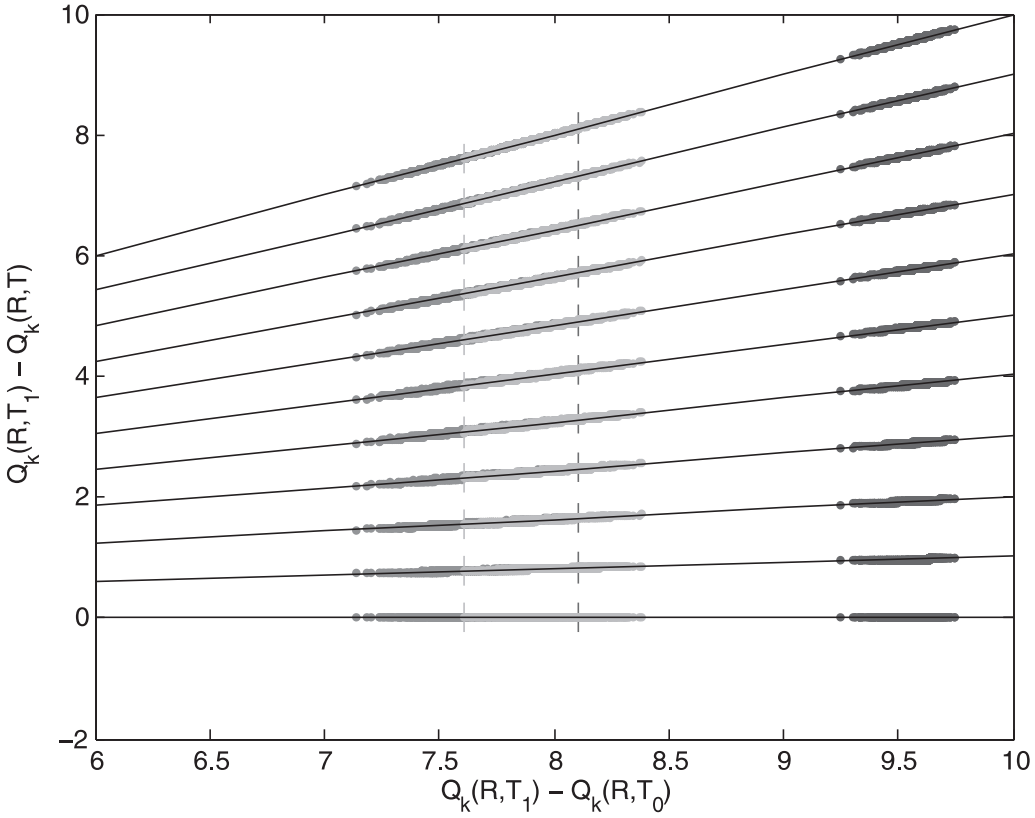

Figure 4.7. A test of the prediction contained in Equation 4.23. According to this equation, the coordinate pairs $(Q_k(R, T_1) - Q_k(R, T_0), Q_k(R, T_1) - Q_k(R, T))$ should, for *all* chips and *all* cone types, fall on a line whose slope depends only on the temperature T of the illuminant, the value of which is that of the function ϕ defined in Equation 4.23. In the figure, we have plotted these log-excitation coordinates for every Munsell chip, over temperatures spaced equally on the mired scale from $T_0 = 4000$ K to $T_1 = 100{,}000$ K. As one would expect, the coordinate pairs for *L*-cones overlap with those of the *M*-cones (as delineated by the dashed lines). In contrast, the *S*-cone coordinate pairs are well separated.

strate with a light source, a red filter, and a 1970s map of the New York City subway system (http://www.nycsubway.org/perl/caption.pl?/img/maps/system_1972.jpg).

References

Finlayson, G. D., Drew, M. S., & Funt, B. F. (1994). Color constancy: Generalized diagonal transforms suffice. *Journal of the Optical Society of America A: Optics, Image Science, and Vision, 11,* 3011–3019. doi:10.1364/JOSAA.11.003011

Finlayson, G. D., & Hordley, S. D. (2001). Color constancy at a pixel. *Journal of the Optical Society of America A: Optics, Image Science, and Vision, 18,* 253–264. doi:10.1364/JOSAA.18.000253

Forsyth, D. A. (1994). Colour constancy. In A. Blake & T. Troscianko (Eds.), *AI and the eye* (pp. 201–228). Chichester, England: Wiley.

Foster, D. H., & Nascimento, S. M. C. (1994). Relational color constancy from invariant cone-excitation ratios. *Proceedings. Biological Sciences, 257,* 115–121. doi:10.1098/rspb.1994.0103

Golz, J., & MacLeod, D. I. A. (2002, February 7). Influence of scene statistics on color constancy. *Nature, 415,* 637–640. doi:10.1038/415637a

Lamb, T. D. (1995). Photoreceptor spectral sensitivities: Common shape in the long-wavelength region. *Vision Research, 35,* 3083–3091. doi:10.1016/0042-6989(95)00114-F

Lamb, T. D. (1999). Photopigments and the biophysics of transduction in cone photoreceptors. In K. R. Gegenfurtner & L. T. Sharpe (Eds.), *Color vision* (pp. 89–101). New York, NY: Cambridge University Press.

MacLeod, D. I. A., & Boynton, R. M. (1979). Chromaticity diagram showing cone excitation by stimuli of equal luminance. *Journal of the Optical Society of America A: Optics and Image Science, 69,* 1183–1186.

MacLeod, D. I. A., & Golz, J. (2003). A computational analysis of colour constancy. In R. Mausfeld & D. Heyer (Eds.), *Color perception: Mind and the physical world* (pp. 205–242). Oxford, England: Oxford University Press. doi:10.1093/acprof:oso/9780198505006.003.0007

Mansfield, R. J. W. (1985). Primate photopigments and cone mechanisms. In A. Fein & J. S. Levine (Eds.), *The visual system* (pp. 89–106). New York, NY: Liss.

Marchant, J. A., & Onyango, C. M. (2001). Color invariant for daylight changes: Relaxing the constraints on illuminants. *Journal of the Optical Society of America A: Optics, Image Science, and Vision, 18,* 2704–2706. doi:10.1364/JOSAA.18.002704

Marchant, J. A., & Onyango, C. M. (2002). Spectral invariance under daylight illumination changes. *Journal of the Optical Society of America A: Optics, Image Science, and Vision, 19,* 840–848. doi:10.1364/JOSAA.19.000840

Sharpe, L. T., Stockman, A., Jägle, H., & Nathans, J. (1999). Opsin genes, cone photopigments, color vision, and color blindness. In K. R. Gegenfurtner & L. T. Sharpe (Eds.), *Color vision* (pp. 3–51). Cambridge, England: Cambridge University Press.

Stockman, A., & Sharpe, L. T. (2000). Spectral sensitivities of the middle- and long-wavelength sensitive cones derived from measurements in observers of known genotype. *Vision Research, 40,* 1711–1737. doi:10.1016/S0042-6989(00)00021-3

Stockman, A., Sharpe, L. T., & Fach, C. (1999). The spectral sensitivity of the human short-wavelength cones derived from thresholds and color matches. *Vision Research, 39,* 2901–2927. doi:10.1016/S0042-6989(98)00225-9

Wyszecki, G., & Stiles, W. S. (1982). *Color science: Concepts and methods, quantitative data and formulae* (2nd ed.). New York, NY: Wiley.